

Formation of a bimetallic Ti–Al material by a wire-feed electron-beam additive manufacturing

© 2023

Andrey V. Luchin*¹, postgraduate student,
research engineer of “Physics of Hierarchical Structures of Metals and Alloys” Laboratory
Elena G. Astafurova², Doctor of Sciences (Physics and Mathematics), Associate Professor,
chief researcher of “Physics of Hierarchical Structures of Metals and Alloys” Laboratory
Sergey V. Astafurov³, PhD (Physics and Mathematics),
senior researcher of “Physics of Hierarchical Structures of Metals and Alloys” Laboratory
Kseniya A. Reunova⁴, postgraduate student,
junior researcher of “Physics of Hierarchical Structures of Metals and Alloys” Laboratory
Elena A. Zagibalova⁵, student, engineer of “Physics of Hierarchical Structures of Metals and Alloys” Laboratory
Eugeny A. Kolubaev⁶, Doctor of Sciences (Engineering), Professor, Director
Institute of Strength Physics and Materials Science of Siberian Branch of Russian Academy of Sciences, Tomsk (Russia)

*E-mail: luchin250398@yandex.ru¹ORCID: <https://orcid.org/0000-0003-4020-0755>²ORCID: <https://orcid.org/0000-0002-1995-4205>³ORCID: <https://orcid.org/0000-0003-3532-3777>⁴ORCID: <https://orcid.org/0000-0002-1318-1010>⁵ORCID: <https://orcid.org/0000-0002-2079-7198>⁶ORCID: <https://orcid.org/0000-0001-7288-3656>

Received 20.06.2023

Accepted 21.08.2023

Abstract: Currently, there is a request from aerospace and aircraft for the construction materials with sufficiently high mechanical strength, thermal creep, corrosion and oxidation resistance. The conventional alloys used for these purposes are too heavy. At the same time, alternative light materials such as Ti–Al-based alloys have many flaws, when they are produced by conventional methods. This work considers the possibility to produce the Ti–Al-based alloys by the method of a wire-feed electron-beam additive manufacturing (EBAM). We study the chemical and phase compositions, microstructure and microhardness of a bimetallic Ti–Al alloy, obtained by this method. It is found the formation of five characteristic regions between titanium and aluminum parts of the bimetallic billet. The mixing zone consists of TiAl and TiAl₃ intermetallics, that is confirmed by the investigation of microstructure, chemical and phase compositions. According to XRD (X-ray diffraction) and EDS (energy-dispersive X-ray spectroscopy) analyses, it can be assumed that TiAl intermetallic prevails over TiAl₃ one. The average microhardness of the mixing zone equals to 450 HV (≈ 4.4 GPa). This zone has developed dendritic microstructure, and even distribution of the phases without link to dendritic and inter-dendritic zones. The cracks appearing in this area are filled with the material of the upper layers, so the whole material is poreless and defect-free. Thus, the results of this work have shown a fundamental possibility to produce the intermetallic Ti–Al alloys with the use of the EBAM.

Keywords: electron beam additive manufacturing; titanium aluminide; Ti–Al; TiAl₃; titanium; aluminum; intermetallics; microstructure; microhardness.

Acknowledgements: The work was supported by the Government research assignment for Institute of Strength Physics and Materials Science SB RAS, project No. FWRW-2022-0005.

The equipment of the “Nanotech” center of the Institute of Strength Physics and Materials Science SB RAS was utilized.

The authors thank V. Rubtsov and S. Nikonov for their assistance with the additive manufacturing of the material.

The paper was written on the reports of the participants of the XI International School of Physical Materials Science (SPM-2023), Togliatti, September 11–15, 2023.

For citation: Luchin A.V., Astafurova E.G., Astafurov S.V., Reunova K.A., Zagibalova E.A., Kolubaev E.A. Formation of a bimetallic Ti–Al material by a wire-feed electron-beam additive manufacturing. *Frontier Materials & Technologies*, 2023, no. 3, pp. 61–70. DOI: 10.18323/2782-4039-2023-3-65-6.

INTRODUCTION

Conventional alloys used for aerospace and turbine engines are superalloys based on Ni, Co, or Fe. They provide sufficient mechanical strength, high thermal creep, corrosion and oxidation resistance [1]. All of these groups of alloys have a quite high value of density, that influences the efficiency in terms of sensible lifting force usage, fuel waste and CO₂ emission as a result [2]. Hence, there is an obvious question about the possibility of obtaining such

alternative alloys that would be light enough and have all the aforementioned properties.

Low density (≈ 3.8 g/cm³), good resistance to high temperature creep, and oxidation are essential properties of Ti–Al-based alloys, which take note attention of the aerospace, aircraft and automotive industries. These alloys have a significantly higher specific yield strength compared to conventional alloys such as Ti and Ni-based alloys, especially in the temperature range of 600–1000 °C [3]. In addition, TiAl intermetallic has a slight advantage in cost and density

compared to Ti-alloys, which average density is $\approx 4.5 \text{ g/cm}^3$ [1]. The intermetallic can also compete in value of density, strength and possible exploiting temperatures with traditional Al-based alloys applied in aircraft industry [4]. The main disadvantage of TiAl intermetallic constraining it from widespread usage was low plasticity (less 2 %) at room temperature [5]. Although there were approaches to improve plasticity by severe plastic deformation and thermal treatment, which included: strengthening by nanotwins or precipitates, formation of nanograin gradient structure or a bimodal microstructure [6]. The use of these mechanisms allows to achieve strain to failure of $\approx 14 \%$ in TiAl intermetallics. Moreover, understanding of phase transformations, and use of thermal treatment enabled the start of application of Ti–Al-based alloys in automobile and aircraft industries [7; 8].

Conventional fabrication and processing of Ti–Al-based alloys have a range of difficulties. The most cost-effective way of fabrication is casting, but this method delivers the coarse-grained lamellar samples with high anisotropy and well-known flaws [9–11]. There is a study where authors overcame the disadvantages of casting by selection of temperatures, cooling rates and crucible materials. They succeed in obtaining a homogeneous structure without macroscopic defects, although some protrusions on the surface have been detected, and there was a need for post processing [12]. Obviously, such quality of products is unacceptable for aircraft and aerospace applications.

Other conventional methods such as powder metallurgy, and wrought processing (rolling, forging, extrusion) have many drawbacks. Their common disadvantage is the large working cycle of machining to obtain the required accuracy and shape of the parts. The additional machining also leads to the need for heat treatments and waste of material. Powder metallurgy is always related to high porosity, oxygen impurities, low plasticity, and additional processing requirement [13].

Currently, researchers try to find the best production way of the intermetallic in the field of additive manufacturing (AM) methods. The main advantages of AM technologies are cost-effectiveness (there is no need for additional machining with waste material), high dimensional accuracy and variability of the shape of the parts. These methods can be divided into three main groups in terms of a feedstock usage: a wire-feed AM, a powder-feed AM, and a powder bed fusion AM [13–15]. The first two allow obtaining parts in the wide size range with high building rates, when the third is not suitable for large parts but has good dimensional accuracy, and lower surface roughness. The last method has an important disadvantage, regardless of which heat source is used (laser or electron beam). The problem is the high temperature gradient, and the cooling rate of the material in the process. This leads to an inhomogeneous structure with a lot of cracks [13–15]. Although some researchers suggest numerical thermokinetic models of a layer growth that allow to optimize the process of powder melting. It is shown that the scanning mode, in particular the electron beam scanning step, most of all affects the quality of the surface layer [16].

The choice of electron beam as a source of energy is optimal in terms of price, stability and control of the AM process in comparison with laser beam and arc. The performance executing in a vacuum, that is necessary during

the working of titanium, delivers a high purity of a resulting product [17; 18].

The use of wires as a feedstock allows to minimise the quantity of impurities and pores, and avoid the structural inhomogeneity as a result. This approach also has a bigger potential in terms of its use in industry, because of the assortment, availability and quality of wires are significantly greater than those for powders [19; 20].

The work is aimed to consider the possibility to produce Ti–Al-based alloys by the method of a wire-feed electron-beam additive manufacturing. We study the chemical and phase compositions, microstructure and microhardness of the additively obtained bimetallic material, with the focus on the transition zone between the Ti- and Al-based parts.

METHODS

The bimetallic billet presented in Fig. 1 a was fabricated by the method of a wire-feed electron beam additive manufacturing. The installation for electron-beam additive manufacturing (EBAM) consisted of a vacuum chamber, a wire feeder, an electron beam source and a movable three-axis table. It was engineered in the Institute of Strength Physics and Materials Science (Siberian Branch of the Russian Academy of Sciences). The feedstock was presented by two kinds of wires. The materials of wires were titanium (Grade 2; Ti–0.25Fe–0.2H–0.2O–0.1Si–0.07C–N0.04) and aluminium (EN ISO 18273; 99.8Al–0.13Fe–0.01Cu–0.01Mn–0.02Si–0.01V). A diameter of wires was 1.2 mm for both materials. The billet moved and melted under an electron beam along a substrate made of a mild steel. The chemical composition of the steel was Fe–1.9Mn–0.8Si–0.08C wt. %. The change of Z-coordinate and rotation by 180° occurred for each next layer. The first 14 applied layers were made of titanium wire, and then the material changed and to 14 layers of aluminium were deposited. An approximate height of each layer in the resultant billet was about 0.5 mm. During the process, a beam current was changing from 55 to 33 mA for titanium layers, and from 13 to 16 mA for aluminium ones. A scanning frequency and a wire feed rate were 100 Hz and 5.8 mm/s respectively. The process of EBAM was carried out in a vacuum chamber at a pressure of 10^{-3} Pa. The studied sample with dimensions of $13 \times 7 \times 1$ mm in size shown in Fig. 1 b was cut off a billet by electrical discharge machining.

The sample was mechanically ground and polished. The solution consisted of hydrofluoric acid, nitric acid, and water in the proportion of 25:7:3 was used for etching of the sample. Microstructure and surface morphology of the sample were studied on Apreo 2 SEM scanning electron microscope (SEM, Thermo Fisher Scientific, Czech Republic) in back-scattered electrons (BSE) mode. LEO EVO 50 SEM (Zeiss, Germany) with an energy dispersive spectroscopy (EDS) device was used for elemental composition analysis. The definition of phase composition of the specimens was performed by X-ray diffraction on DRON 7 diffractometer (Bourestnik, Saint Petersburg, Russia) with Co-K α radiation. XRD analysis was performed for the section cut in parallel to the substrate in the intermediate between Ti and Al regions highlighted with a dashed line in Fig. 2. AFFRI DM8 microhardness tester (Affri, Italy) was applied for rough assessment of mechanical properties. The load on the Vickers indenter was 100 g, and a load time of 10 s was used.

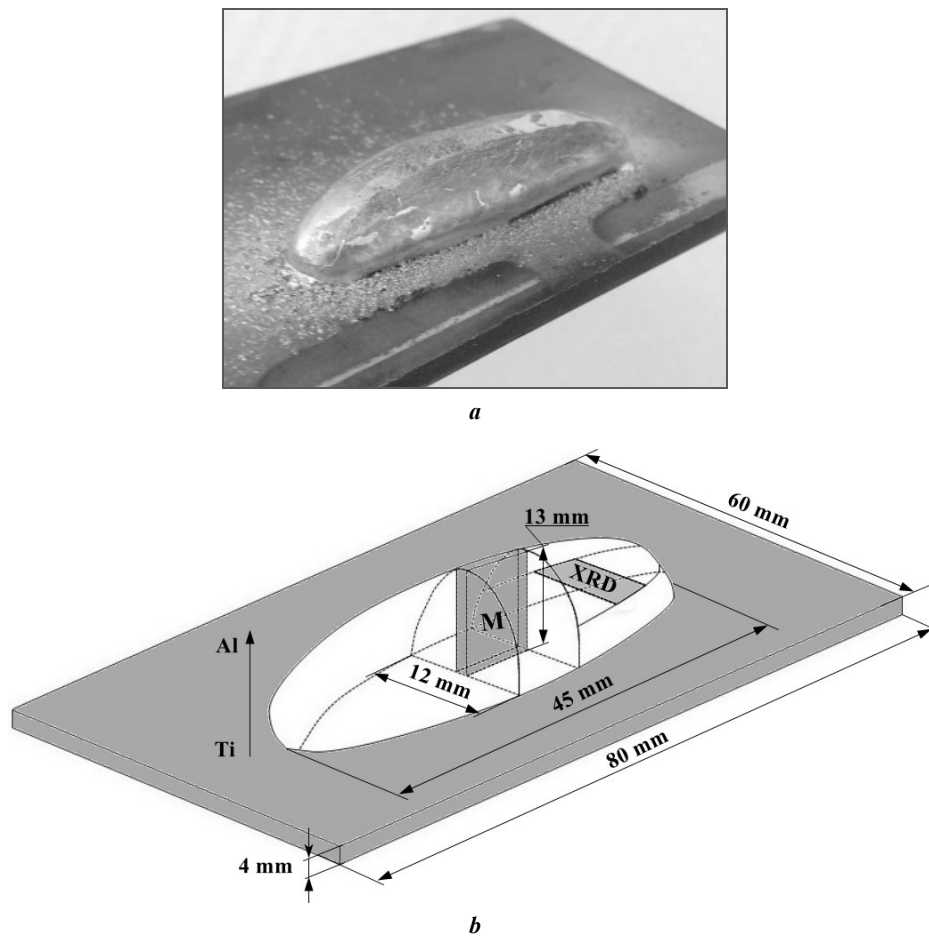


Fig. 1. EBAM-fabricated Ti–Al alloy billet (a) and extracted sections for study of the microstructure (M) and phase composition (PCA) (b)
Рис. 1. Заготовка сплава Ti–Al, полученная методом ЭЛАП (a), и сечения, выбранные для исследования микроструктуры (M) и фазового состава (PCA) (b)

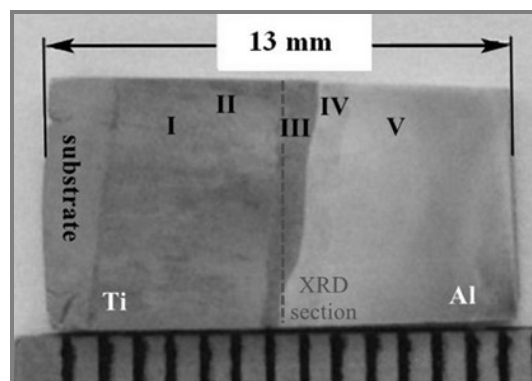


Fig. 2. The common view of the studied sample extracted from the EBAM-fabricated bimetallic billet as shown in Fig. 1 b. Numbers I, II, III, IV, V show characteristic zones revealed by etching of the sample.

I – the zone of the titanium layer near the substrate material where their mixing is realized;

II – the part of the titanium layer located next to the mixing zone of titanium and aluminum;

III – the mixing zone of the Ti and Al components in the melting pool;

IV – the intermediate layer between the mixing zone and the region of pure aluminum

Рис. 2. Общий вид исследуемого образца, извлеченного из биметаллической заготовки, полученной методом ЭЛАП и показанной на рис. 1 б. Цифры I, II, III, IV, V обозначают характерные зоны, выявленные травлением образца.

I – зона слоя титана вблизи материала подложки, где осуществляется их смешивание;

II – часть титанового слоя, расположенная рядом с зоной смешивания титана и алюминия;

III – зона смешивания компонентов Ti и Al в плавильной ванне;

IV – промежуточный слой между зоной смешивания и областью чистого алюминия; V – слои чистого алюминия

RESULTS

Fig. 2 presents the metallographic image of the studied sample extracted from the EBAM-fabricated bimetallic billet. The difference of tones from dark-grey of Ti to light-grey of Al is seen after etching of the sample. Area I is defined as the zone of the titanium layer near the substrate material where their mixing is realised. Area II is the part of the titanium layer located next to the mixing zone of titanium and aluminium. The mixing zone marked as area III corresponds to the mixture of the Ti and Al components in the melting pool. Area IV was defined as the intermediate layer between the mixing zone and the region of pure aluminium. The last region is presented by the layers of pure aluminium and corresponds to area V.

Areas V and I are the furthest regions from the mixing zone, and their compositions correspond to the wire materials made of pure aluminium and titanium, respectively. Since the mixing zone and the nearest regions are the main area of interest, the elemental composition analysis for areas V and I was not performed. According to EDS data, the elemental composition of area VI is presented by aluminium, titanium is almost absent (<1 %) (Table 1). Area III contains high values of Al ($\approx 52\%$) and Ti ($\approx 44\%$). According to TiAl phase diagram such ratio of components can match γ -TiAl phase. SEM-image of microstructure shows that there are cracks filled with aluminium layers in the mixing zone (Fig. 3 a). It is noticeable that area III has developed dendritic microstructure (Fig. 3 b). The absence of a composition contrast in BSE mode of SEM-imaging shows the even distribution of the phases without link to dendritic and inter-dendritic zones. Thus, area III is more attractive and takes attention in terms of finding Ti–Al compositions. Because of that, the further research is focused on this area. Area II contains the significant volume of titanium ($\approx 90\text{--}92\%$) and iron ($\approx 7\text{--}9\%$), but aluminium is almost absent (<1 %).

According to XRD pattern of EBAM-fabricated sample in area III, the phase composition is presented by TiAl and TiAl₃ phases (Fig. 4). The small peak corresponded to 41.5° (111) can be explained only by the presence of insignificant quantity of α -Ti phase. The intensity of the peaks, especially the first two most intensive peaks of 45.0° (111) and 52.4° (002), shows that TiAl intermetallic noticeably prevails over TiAl₃. In addition, we can not deny the presence of aluminium since it has common peaks with TiAl intermetallic phase.

Since the interfaces between the areas II, III, and IV are not flat, the Ti and Al layers adjacent to area III are in the field of X-ray analysis. Due to this, the α -Ti phase stabilised by aluminium from the upper regions of area IV appears in area III. At the same time, stabilization of the β -Ti phase is observed in area II due to the presence of iron diffusing from the substrate (Fig. 5, Table 1).

Microhardness of EBAM-fabricated bimetallic Ti–Al alloy sample varies throughout the whole billet. This means the significant difference of strength properties of all its areas (Fig. 6).

The microhardness of areas I and II is ≈ 530 HV (≈ 5.2 GPa) and ≈ 390 HV (≈ 3.8 GPa), respectively. The average value of microhardness for area III is 450 HV (≈ 4.4 GPa). There is a region related to area IV with devia-

tion from the μ H value of pure aluminium where the microhardness is about 70 HV. The value of aluminium layer corresponded to area V equals to 30 HV.

DISCUSSION

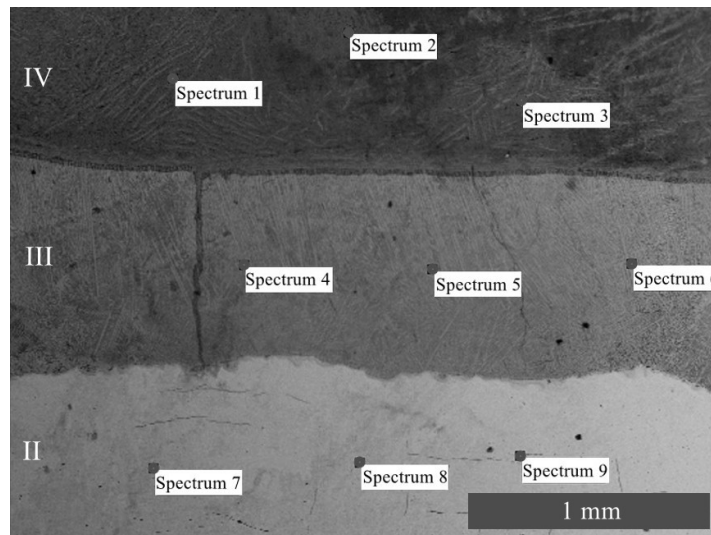
As it was shown above in Fig. 2, the EBAM method allowed to obtain the bimetallic billet of Ti–Al system. Various regions can be easily distinguished by their grey shades into five characteristic areas, with different chemical and phase compositions. The microhardness testing results also allow to differ them by the noticeable changes of microhardness along the height of the sample.

The first deposited layers, related to areas I and II, are supposed to the initial phase composition of Grade 2 titanium wire presented by α -Ti phase. But the microhardness values of these areas are significantly higher than usual for Grade 2 pure titanium consisted of α -Ti phase (≈ 1.5 GPa) [21]. It is shown that, according to the results of XRD analysis, area II is presumably presented by β -Ti solution (Fig. 5). The formation of β -Ti phase in pure titanium is possible, when the temperature of heat treatment achieves the point of phase transformation equal to ≈ 590 °C, with following quenching [22]. The temperature of melting pool achieved by the EBAM process is significantly higher than 590 °C, but the cooling rate is quite low [23]. This means that the phase composition will be presented by the α -Ti phase as a result. Although, the presence of iron in these areas confirmed by the EDS data is high, and sufficient for preventing of the α -Ti-phase formation, since iron is a strong stabilizer of the β -phase [24]. The increase of microhardness values occurring from area II to area I in the direction of the substrate should be related to the change of chemical and phase composition [25]. According to phase diagram of the Fe–Ti system this can be a result of FeTi-intermetallic appearance [22]. An increase in the concentration of iron, in the direction of the substrate, contributes to an increase in the volume of the intermetallic phase, and hence the strength characteristics.

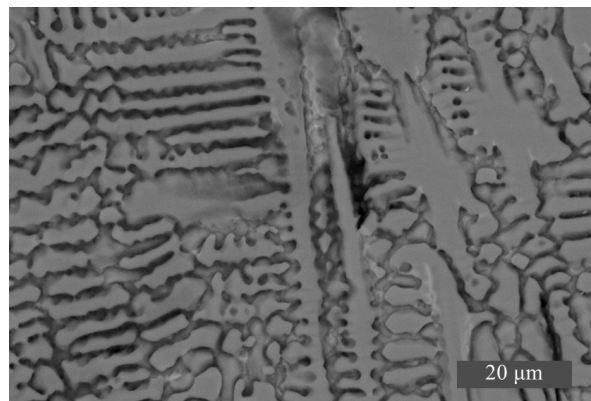
The EDS data of area III, shows a small deviation from equiatomic ratio between aluminium and titanium components to the side of the former (Table 1). The XRD analysis confirms that obtained alloy in this area is presented by TiAl and TiAl₃ intermetallics, Al, and α -Ti phases (Fig. 4). Presumably the presence of aluminium in area III, provides the small appearance of α -Ti phase, since the former contributes stabilisation of α -Ti phase [24]. Moreover, the pure Al can be detected in this area because of filling the cracks with the aluminium (Fig. 3 a). When the layers in the area III solidified, the material of the upper aluminium layer of area IV filled these cracks. Thus, there is the process of the "healing" of these cracks which appear in area III while the following deposition. Due to this, there are no voids or cracks in the mixing zone. It is also obvious that a quantity of the aluminium phase in this area should not be large. This follows from the fact that, according to EDS data, the quantity of titanium is large, and cannot be presented only by the trace amount of α -Ti phase. The average value of microhardness in area III is 450 HV (≈ 4.4 GPa) and corresponds to the possible range from 3 GPa to 5 GPa for TiAl-based intermetallics (Fig. 6) [26]. This range is quite wide, because the microhardness depends on the microstructure,

Table 1. EDS data for areas II, III, IV of the EBAM-fabricated Ti–Al alloy sample
Таблица 1. Результаты ЭДС для областей II, III, IV сплава Ti–Al, полученного методом ЭЛАП

Area	Spectrum	Al	Ti	Fe
		Atomic %		
IV	1	99.87	0.11	0.02
	2	99.99	0.01	0.00
	3	99.80	0.11	0.09
III	4	52.55	42.83	4.62
	5	57.07	40.96	1.97
	6	58.15	38.85	3.00
II	7	0.06	90.70	9.24
	8	0.89	91.40	7.71
	9	0.24	92.45	7.31



a



b

Fig. 3. SEM-image of microstructure and EDS points for areas II, III, IV (a) and BSE mode SEM-image of area III (b) of the EBAM-fabricated Ti–Al alloy sample
Рис. 3. СЭМ-изображение микроструктуры и точек ЭДС для областей II, III, IV (a) и СЭМ-изображение в режиме ОРЭ области III сплава Ti–Al, полученного методом ЭЛАП (b)

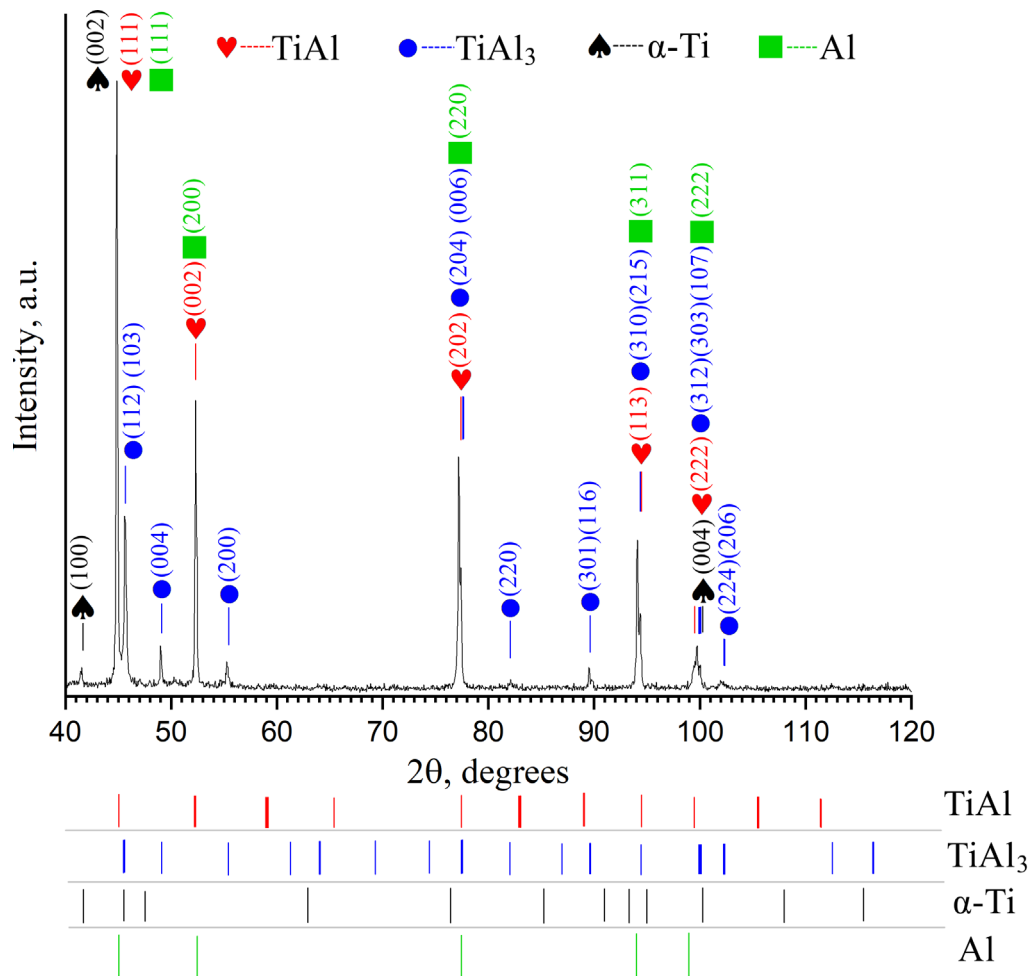


Fig. 4. XRD pattern of EBAM-fabricated bimetallic Ti–Al alloy sample in area III

Рис. 4. РДА-дифрактограмма области III образца биметаллического Ti–Al сплава, полученного методом ЭЛАП

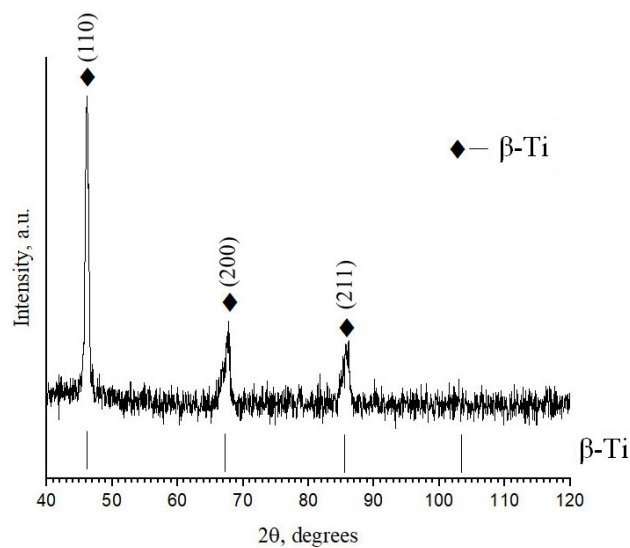


Fig. 5. XRD pattern of EBAM-fabricated sample in area II

Рис. 5. РДА-дифрактограмма области II образца, полученного методом ЭЛАП

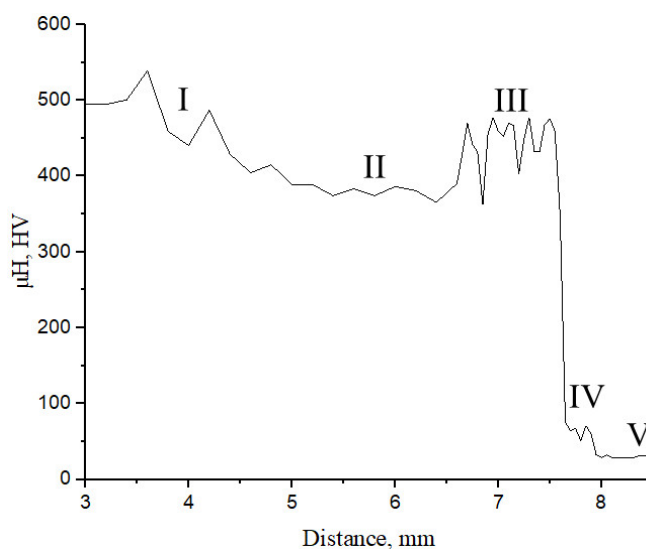


Fig. 6. Microhardness vs the distance from the substrate of EBAM-fabricated sample
Рис. 6. Зависимость микротвердости от расстояния от подложки образца, полученного методом ЭЛАП

exact phase composition stoichiometry and elemental composition. Moreover, it is extremely difficult to obtain homogenous single phase intermetallic. Thus, the phase composition of this area is commonly presented by the mixture of TiAl and TiAl₃ intermetallics, and the former one prevails over the latter.

Area IV was defined as the intermediate layer between the mixing zone and the region of pure aluminium marked as area V. According to EDS data, the elemental composition of area IV is presented by aluminium, titanium is almost absent (<1 %) (Table 1). As it was aforementioned, the microhardness of area IV is higher than typical for pure aluminium (Fig. 6). This can be related to the formation of a small transition zone between area III and pure aluminium layer of area V. Possibly, this zone is the mechanical mixture of pure aluminium and TiAl₃ intermetallic and the Al-based solid solution Al (Ti). Although the zone is quite small and, apparently, does not correspond to the EDS data presented for area IV. Thus, this zone requires more precise study of the chemical and phase composition. Since the microhardness of area V equals to that of pure aluminium, it can be suggested that area V has the same chemical composition [27].

CONCLUSIONS

The possibility to produce Ti–Al-based alloys by the method of a wire-feed electron-beam additive manufacturing is presented in this study. The chemical and phase compositions, microstructure and microhardness of the additively obtained bimetallic material Ti–Al system, with the focus on the transition zone between the Ti- and Al-based parts are carried out.

The method allows us to obtain Ti–Al-based alloy presented by the mixture of TiAl, TiAl₃ intermetallics and an insignificant amount of pure aluminium and titanium phases. The intensity of XRD peaks, the chemical composition ratio, and the value of microhardness show that TiAl

intermetallic noticeably prevails over TiAl₃. The average microhardness of the mixing zone is 450 HV (≈ 4.4 GPa). This zone has developed a dendritic microstructure, and even distribution of the phases without link to dendritic and inter-dendritic zones. The cracks appearing in this area are filled with the material of the upper layers. Thus, the whole material of obtained bimetallic material is defect-free. Although the fact of iron presence from the substrate material in the billet layers requires changing and optimizing of EBAM mode for obtaining of a high-quality bimetallic billet.

REFERENCES

- Gialanella S., Malandrucolo A. Chapter 4. Titanium and Titanium Alloys. *Aerospace alloys*. Switzerland, Springer Publ., 2020, pp. 129–189. DOI: [10.1007/978-3-030-24440-8](https://doi.org/10.1007/978-3-030-24440-8).
- Rao K.A. Nickel Based Superalloys – Properties and Their Applications. *International Journal of Management, Technology and Engineering*, 2018, vol. 8, no. V, pp. 268–277.
- Clemens H., Smarsly W., Güther V., Mayer S. Advanced intermetallic titanium aluminides. *Proceedings of the 13th World Conference on Titanium*, 2016, pp. 1189–1200. DOI: [10.1002/9781119296126.ch203](https://doi.org/10.1002/9781119296126.ch203).
- Dwivedi P., Siddiquee A.N., Maheshwari S. Issues and requirements for aluminum alloys used in aircraft components: state of the art. *Russian Journal of Non-Ferrous Metals*, 2021, vol. 62, pp. 212–225. DOI: [10.3103/S1067821221020048](https://doi.org/10.3103/S1067821221020048).
- Bewlay B.P., Nag S., Suzuki A., Weimer M.J. TiAl alloys in commercial aircraft engines. *Materials at High Temperatures*, 2016, vol. 33, no. 4-5, pp. 549–559. DOI: [10.1080/09603409.2016.1183068](https://doi.org/10.1080/09603409.2016.1183068).
- Edalati K., Toh S., Iwaoka H., Watanabe M., Horita Z., Kashioka D., Kishida K., Inui H. Ultrahigh strength and high plasticity in TiAl intermetallics with bimodal grain

- structure and nanotwins. *Scripta Materialia*, 2012, vol. 67, no. 10, pp. 814–817. DOI: [10.1016/j.scriptamat.2012.07.030](https://doi.org/10.1016/j.scriptamat.2012.07.030).
7. Tetsui T. Application of TiAl in a turbocharger for passenger vehicles. *Advanced Engineering Materials*, 2001, vol. 3, no. 5, pp. 307–310. DOI: [10.1002/1527-2648\(200105\)3:5<307::AID-ADEM307>3.0.CO;2-3](https://doi.org/10.1002/1527-2648(200105)3:5<307::AID-ADEM307>3.0.CO;2-3).
 8. Jarvis D.J., Voss D. IMPRESS Integrated Project – an overview paper. *Materials Science and Engineering: A*, 2005, vol. 413-414, pp. 583–591. DOI: [10.1016/j.msea.2005.09.066](https://doi.org/10.1016/j.msea.2005.09.066).
 9. Clemens H., Kestler H. Processing and applications of intermetallic γ -TiAl-based alloys. *Advanced engineering materials*, 2000, vol. 2, no. 9, pp. 551–570. DOI: [10.1002/1527-2648\(200009\)2:9<551::AID-ADEM551>3.0.CO;2-U](https://doi.org/10.1002/1527-2648(200009)2:9<551::AID-ADEM551>3.0.CO;2-U).
 10. Wu X. Review of alloy and process development of TiAl alloys. *Intermetallics*, 2006, vol. 14, no. 10-11, pp. 1114–1122. DOI: [10.1016/j.intermet.2005.10.019](https://doi.org/10.1016/j.intermet.2005.10.019).
 11. Cobbinah P.V., Matizamhuka W.R. Solid-state processing route, mechanical behaviour, and oxidation resistance of TiAl alloys. *Advances in Materials Science and Engineering*, 2019, vol. 2019, pp. 1–21. DOI: [10.1155/2019/4251953](https://doi.org/10.1155/2019/4251953).
 12. Brotzu A., Felli F., Mondal A., Pilone D. Production issues in the manufacturing of TiAl turbine blades by investment casting. *Procedia Structural Integrity*, 2020, vol. 25, pp. 79–87. DOI: [10.1016/j.prostr.2020.04.012](https://doi.org/10.1016/j.prostr.2020.04.012).
 13. Soliman H.A., Elbestawi M. Titanium aluminides processing by additive manufacturing – a review. *The International Journal of Advanced Manufacturing Technology*, 2022, vol. 119, no. 9-10, pp. 5583–5614. DOI: [10.1007/s00170-022-08728-w](https://doi.org/10.1007/s00170-022-08728-w).
 14. Emiralioğlu A., Ünal R. Additive manufacturing of gamma titanium aluminide alloys: a review. *Journal of Materials Science*, 2022, vol. 57, no. 7, pp. 4441–4466. DOI: [10.1007/s10853-022-06896-4](https://doi.org/10.1007/s10853-022-06896-4).
 15. Dzogbewu T.C. Additive manufacturing of TiAl-based alloys. *Manufacturing Review*, 2020, vol. 7, no. 35, pp. 1–8. DOI: [10.1051/mfreview/2020032](https://doi.org/10.1051/mfreview/2020032).
 16. Kryukova O.N., Knyazeva A.G. Thermokinetic. Model of a Layer Growth on a Substrate During Electron-Beam Cladding. *Russian Physics Journal*, 2023, vol. 66, no. 1, pp. 66–73. DOI: [10.1007/s11182-023-02906-3](https://doi.org/10.1007/s11182-023-02906-3).
 17. Löber L., Biamino S., Ackelid U., Sabbadini S., Epicoco P., Fino P., Eckert J. Comparison off selective laser and electron beam melted titanium aluminides. *International Solid Freeform Fabrication Symposium*, 2011. DOI: [10.26153/tsw/15316](https://doi.org/10.26153/tsw/15316).
 18. Negi S., Nambolan A.A., Kapil S., Joshi P.S., Karunakaran K.P., Bhargava P. Review on electron beam based additive manufacturing. *Rapid Prototyping Journal*, 2020, vol. 26, no. 3, pp. 485–498. DOI: [10.1108/RPJ-07-2019-0182](https://doi.org/10.1108/RPJ-07-2019-0182).
 19. Özel T., Shokri H., Loizeau R. A Review on Wire-Fed Directed Energy Deposition Based Metal Additive Manufacturing. *Journal of Manufacturing and Materials Processing*, 2023, vol. 7, no. 1, article number 45. DOI: [10.3390/jmmp7010045](https://doi.org/10.3390/jmmp7010045).
 20. Kolubaev E.A., Rubtsov V.E., Chumaevsky A.V., Astafurova E.G. Micro-, Meso-and Macrostructural Design of Bulk Metallic and Polymetallic Materials by Wire-Feed Electron-Beam Additive Manufacturing. *Physical Mesomechanics*, 2022, vol. 25, no. 6, pp. 479–491. DOI: [10.1134/S1029959922060017](https://doi.org/10.1134/S1029959922060017).
 21. Lim H.S., Hwang M.J., Jeong H.N., Lee W.Y., Song H.J., Park Y.J. Evaluation of surface mechanical properties and grindability of binary Ti alloys containing 5 wt % Al, Cr, Sn, and V. *Metals*, 2017, vol. 7, no. 11, article number 487. DOI: [10.3390/met7110487](https://doi.org/10.3390/met7110487).
 22. Kriegel M.J., Wetzel M.H., Treichel A., Fabricznaya O., Rafaja D. Binary Ti–Fe system. Part I: Experimental investigation at high pressure. *Calphad*, 2021, vol. 74, article number 102322. DOI: [10.1016/j.calphad.2021.102322](https://doi.org/10.1016/j.calphad.2021.102322).
 23. Osipovich K., Kalashnikov K., Chumaevskii A. et al. Wire-Feed Electron Beam Additive Manufacturing: A Review. *Metals*, 2023, vol. 13, no. 2, article number 279. DOI: [10.3390/ma15030814](https://doi.org/10.3390/ma15030814).
 24. Bieler T.R., Trevino R.M., Zeng L. Alloys: titanium. *Encyclopedia of Condensed Matter Physics*, 2005, pp. 65–76. DOI: [10.1016/B0-12-369401-9/00536-2](https://doi.org/10.1016/B0-12-369401-9/00536-2).
 25. Sujan G.K., Wu B., Pan Z., Li H. In-Situ Fabrication of Titanium Iron Intermetallic Compound by the Wire Arc Additive Manufacturing Process. *Metallurgical and Materials Transactions A*, 2020, vol. 51, pp. 552–557. DOI: [10.1007/s11661-019-05555-9](https://doi.org/10.1007/s11661-019-05555-9).
 26. Chen X.Y., Fang H.Z., Wang Q., Zhang S.Y., Chen R.R., Su Y.Q. Microstructure and microhardness of Ti–48Al alloy prepared by rapid solidification. *China Foundry*, 2020, vol. 17, pp. 429–434. DOI: [10.1007/s41230-020-0090-7](https://doi.org/10.1007/s41230-020-0090-7).
 27. Alshabatat N., Al-qawabah S. Effect of 4 % wt. Cu Addition on the Mechanical Characteristics and Fatigue Life of Commercially Pure Aluminum. *Jordan Journal of Mechanical & Industrial Engineering*, 2015, vol. 9, no. 4, pp. 297–301.

СПИСОК ЛИТЕРАТУРЫ

1. Gialanella S., Malandrucolo A. Chapter 4. Titanium and Titanium Alloys // *Aerospace alloys*. Switzerland: Springer, 2020. P. 129–189. DOI: [10.1007/978-3-030-24440-8](https://doi.org/10.1007/978-3-030-24440-8).
2. Rao K.A. Nickel Based Superalloys – Properties and Their Applications // *International Journal of Management, Technology and Engineering*. 2018. Vol. 8. № V. P. 268–277.
3. Clemens H., Smarsly W., Güther V., Mayer S. Advanced intermetallic titanium aluminides // *Proceedings of the 13th World Conference on Titanium*. 2016. P. 1189–1200. DOI: [10.1002/9781119296126.ch203](https://doi.org/10.1002/9781119296126.ch203).
4. Dwivedi P., Siddiquee A.N., Maheshwari S. Issues and requirements for aluminum alloys used in aircraft components: state of the art // *Russian Journal of Non-Ferrous Metals*. 2021. Vol. 62. P. 212–225. DOI: [10.3103/S1067821221020048](https://doi.org/10.3103/S1067821221020048).
5. Bewlay B.P., Nag S., Suzuki A., Weimer M.J. TiAl alloys in commercial aircraft engines // *Materials at High Temperatures*. 2016. Vol. 33. № 4-5. P. 549–559. DOI: [10.1080/09603409.2016.1183068](https://doi.org/10.1080/09603409.2016.1183068).
6. Edalati K., Toh S., Iwaoka H., Watanabe M., Horita Z., Kashioka D., Kishida K., Inui H. Ultrahigh strength and high plasticity in TiAl intermetallics with bimodal grain structure and nanotwins // *Scripta Materialia*. 2012. Vol. 67. № 10. P. 814–817. DOI: [10.1016/j.scriptamat.2012.07.030](https://doi.org/10.1016/j.scriptamat.2012.07.030).
7. Tetsui T. Application of TiAl in a turbocharger for passenger vehicles // *Advanced Engineering Materials*.

2001. Vol. 3. № 5. P. 307–310. DOI: [10.1002/1527-2648\(200105\)3:5<307::AID-ADEM307>3.0.CO;2-3](https://doi.org/10.1002/1527-2648(200105)3:5<307::AID-ADEM307>3.0.CO;2-3).
8. Jarvis D.J., Voss D. IMPRESS Integrated Project – an overview paper // Materials Science and Engineering: A. 2005. Vol. 413–414. P. 583–591. DOI: [10.1016/j.msea.2005.09.066](https://doi.org/10.1016/j.msea.2005.09.066).
 9. Clemens H., Kestler H. Processing and applications of intermetallic γ -TiAl-based alloys // Advanced engineering materials. 2000. Vol. 2. № 9. P. 551–570. DOI: [10.1002/1527-2648\(200009\)2:9<551::AID-ADEM551>3.0.CO;2-U](https://doi.org/10.1002/1527-2648(200009)2:9<551::AID-ADEM551>3.0.CO;2-U).
 10. Wu X. Review of alloy and process development of TiAl alloys // Intermetallics. 2006. Vol. 14. № 10–11. P. 1114–1122. DOI: [10.1016/j.intermet.2005.10.019](https://doi.org/10.1016/j.intermet.2005.10.019).
 11. Cobbinah P.V., Matizamhuka W.R. Solid-state processing route, mechanical behaviour, and oxidation resistance of TiAl alloys // Advances in Materials Science and Engineering. 2019. Vol. 2019. P. 1–21. DOI: [10.1155/2019/4251953](https://doi.org/10.1155/2019/4251953).
 12. Brotzu A., Felli F., Mondal A., Pilone D. Production issues in the manufacturing of TiAl turbine blades by investment casting // Procedia Structural Integrity. 2020. Vol. 25. P. 79–87. DOI: [10.1016/j.prostr.2020.04.012](https://doi.org/10.1016/j.prostr.2020.04.012).
 13. Soliman H.A., Elbestawi M. Titanium aluminides processing by additive manufacturing – a review // The International Journal of Advanced Manufacturing Technology. 2022. Vol. 119. № 9–10. P. 5583–5614. DOI: [10.1007/s00170-022-08728-w](https://doi.org/10.1007/s00170-022-08728-w).
 14. Emiralioglu A., Ünal R. Additive manufacturing of gamma titanium aluminide alloys: a review // Journal of Materials Science. 2022. Vol. 57. № 7. P. 4441–4466. DOI: [10.1007/s10853-022-06896-4](https://doi.org/10.1007/s10853-022-06896-4).
 15. Dzoğbewu T.C. Additive manufacturing of TiAl-based alloys // Manufacturing Review. 2020. Vol. 7. № 35. P. 1–8. DOI: [10.1051/mfreview/2020032](https://doi.org/10.1051/mfreview/2020032).
 16. Kryukova O.N., Knyazeva A.G. Thermokinetic. Model of a Layer Growth on a Substrate During Electron-Beam Cladding // Russian Physics Journal. 2023. Vol. 66. № 1. P. 66–73. DOI: [10.1007/s11182-023-02906-3](https://doi.org/10.1007/s11182-023-02906-3).
 17. Löber L., Biamino S., Ackelid U., Sabbadini S., Epicoco P., Fino P., Eckert J. Comparison off selective laser and electron beam melted titanium aluminides // International Solid Freeform Fabrication Symposium. 2011. DOI: [10.26153/tsw/15316](https://doi.org/10.26153/tsw/15316).
 18. Negi S., Nambolan A.A., Kapil S., Joshi P.S., Karunakaran K.P., Bhargava P. Review on electron beam based additive manufacturing // Rapid Prototyping Journal. 2020. Vol. 26. № 3. P. 485–498. DOI: [10.1108/RPJ-07-2019-0182](https://doi.org/10.1108/RPJ-07-2019-0182).
 19. Özel T., Shokri H., Loizeau R. A Review on Wire-Fed Directed Energy Deposition Based Metal Additive Manufacturing // Journal of Manufacturing and Materials Processing. 2023. Vol. 7. № 1. Article number 45. DOI: [10.3390/jmmp7010045](https://doi.org/10.3390/jmmp7010045).
 20. Kolubaev E.A., Rubtsov V.E., Chumaevsky A.V., Astafurova E.G. Micro-, Meso- and Macrostructural Design of Bulk Metallic and Polymetallic Materials by Wire-Feed Electron-Beam Additive Manufacturing // Physical Mesomechanics. 2022. Vol. 25. № 6. P. 479–491. DOI: [10.1134/S1029959922060017](https://doi.org/10.1134/S1029959922060017).
 21. Lim H.S., Hwang M.J., Jeong H.N., Lee W.Y., Song H.J., Park Y.J. Evaluation of surface mechanical properties and grindability of binary Ti alloys containing 5 wt % Al, Cr, Sn, and V // Metals. 2017. Vol. 7. № 11. Article number 487. DOI: [10.3390/met7110487](https://doi.org/10.3390/met7110487).
 22. Kriegel M.J., Wetzels M.H., Treichel A., Fabrichnaya O., Rafaja D. Binary Ti–Fe system. Part I: Experimental investigation at high pressure // Calphad. 2021. Vol. 74. Article number 102322. DOI: [10.1016/j.calphad.2021.102322](https://doi.org/10.1016/j.calphad.2021.102322).
 23. Osipovich K., Kalashnikov K., Chumaevskii A. et al. Wire-Feed Electron Beam Additive Manufacturing: A Review // Metals. 2023. Vol. 13. № 2. Article number 279. DOI: [10.3390/ma15030814](https://doi.org/10.3390/ma15030814).
 24. Bieler T.R., Trevino R.M., Zeng L. Alloys: titanium // Encyclopedia of Condensed Matter Physics. 2005. P. 65–76. DOI: [10.1016/B0-12-369401-9/00536-2](https://doi.org/10.1016/B0-12-369401-9/00536-2).
 25. Sujan G.K., Wu B., Pan Z., Li H. In-Situ Fabrication of Titanium Iron Intermetallic Compound by the Wire Arc Additive Manufacturing Process // Metallurgical and Materials Transactions A. 2020. Vol. 51. P. 552–557. DOI: [10.1007/s11661-019-05555-9](https://doi.org/10.1007/s11661-019-05555-9).
 26. Chen X.Y., Fang H.Z., Wang Q., Zhang S.Y., Chen R.R., Su Y.Q. Microstructure and microhardness of Ti–48Al alloy prepared by rapid solidification // China Foundry. 2020. Vol. 17. P. 429–434. DOI: [10.1007/s41230-020-0090-7](https://doi.org/10.1007/s41230-020-0090-7).
 27. Alshabat N., Al-qawabah S. Effect of 4 % wt. Cu Addition on the Mechanical Characteristics and Fatigue Life of Commercially Pure Aluminum // Jordan Journal of Mechanical & Industrial Engineering. 2015. Vol. 9. № 4. P. 297–301.

Формирование биметаллического материала Ti–Al

методом проволочного электронно-лучевого аддитивного производства

© 2023

*Лучин Андрей Владимирович**¹, аспирант,

инженер-исследователь лаборатории физики иерархических структур в металлах и сплавах

*Астафурова Елена Геннадьевна*², доктор физико-математических наук, доцент,

главный научный сотрудник лаборатории физики иерархических структур в металлах и сплавах

*Астафуров Сергей Владимирович*³, кандидат физико-математических наук,

старший научный сотрудник лаборатории физики иерархических структур в металлах и сплавах

*Реунова Ксения Андреевна*⁴, аспирант,

младший научный сотрудник лаборатории физики иерархических структур в металлах и сплавах

*Загibalова Елена Андреевна*⁵, студент,

инженер лаборатории физики иерархических структур в металлах и сплавах

*Колубаев Евгений Александрович*⁶, доктор технических наук, профессор, директор

Институт физики прочности и материаловедения Сибирского отделения Российской академии наук, Томск (Россия)

*E-mail: luchin250398@yandex.ru

¹ORCID: <https://orcid.org/0000-0003-4020-0755>

²ORCID: <https://orcid.org/0000-0002-1995-4205>

³ORCID: <https://orcid.org/0000-0003-3532-3777>

⁴ORCID: <https://orcid.org/0000-0002-1318-1010>

⁵ORCID: <https://orcid.org/0000-0002-2079-7198>

⁶ORCID: <https://orcid.org/0000-0001-7288-3656>

Поступила в редакцию 20.06.2023

Принята к публикации 21.08.2023

Аннотация: В настоящее время в аэрокосмической промышленности и авиастроении существует запрос на новые конструкционные материалы, обладающие достаточно высокой механической прочностью, тепловой ползучестью, стойкостью к коррозии и окислению. Обычные сплавы, используемые для этих целей, слишком тяжелы. В то же время альтернативные легкие материалы, такие как сплавы на основе Ti–Al, имеют множество недостатков при производстве традиционными методами. В данной работе рассмотрена возможность получения сплавов на основе Ti–Al методом проволочного электронно-лучевого аддитивного производства (ЭЛАП). Изучены химический и фазовый составы, микроструктура и микротвердость биметаллического сплава Ti–Al, полученного данным методом. Обнаружено образование пяти характерных областей между титановой и алюминиевой частями биметаллической заготовки. Зона смешивания состоит из интерметаллидов TiAl и TiAl₃, что подтверждается исследованием ее микроструктуры, химического и фазового составов. По результатам рентгеновского дифракционного анализа и энергодисперсионной рентгеновской спектроскопии можно предположить, что объемная доля интерметаллида TiAl в зоне смешивания выше, чем доля фазы TiAl₃. Средняя микротвердость зоны смешивания составляет 450 HV ($\approx 4,4$ ГПа). В зоне смешивания сформировалась развитая дендритная микроструктура и равномерное распределение фаз без привязки к дендритным и междендритным зонам. Трещины, появляющиеся в этой области, заполняются материалом верхних слоев, поэтому материал беспористый и бездефектный. Это показывает принципиальную возможность получения интерметаллидных сплавов Ti–Al с использованием ЭЛАП.

Ключевые слова: электронно-лучевое аддитивное производство; алюминид титана; Ti–Al; TiAl₃; титан; алюминий; интерметаллиды; микроструктура; микротвердость.

Благодарности: Работа выполнена в рамках государственного научного задания Института физики прочности и материаловедения СО РАН, проект № FWRW-2022-0005).

Исследования выполнены с использованием оборудования Центра коллективного пользования «Нанотех» Института физики прочности и материаловедения СО РАН.

Авторы благодарят Рубцова В.Е. и Никонова С.Ю. за помощь при аддитивном производстве материала.

Статья подготовлена по материалам докладов участников XI Международной школы «Физическое материаловедение» (ШФМ-2023), Тольятти, 11–15 сентября 2023 года.

Для цитирования: Лучин А.В., Астафурова Е.Г., Астафуров С.В., Реунова К.А., Загибалова Е.А., Колубаев Е.А. Формирование биметаллического материала Ti–Al методом проволочного электронно-лучевого аддитивного производства // *Frontier Materials & Technologies*. 2023. № 3. С. 61–70. DOI: 10.18323/2782-4039-2023-3-65-6.